
ONLINE GRADIENT DESCENT FOR FLEXIBLE POWER POINT TRACKING UNDER A HIGHLY FLUCTUATING WEATHER AND LOAD

A PREPRINT

Muhy Eddin Za'ter
Electrical and Computer Engineering
University of Colorado Boulder
muhy.zater@colorado.edu

Abdallah Adwan
Electrical Engineering Department
Oregon Institute of Technology
abdallah.adwan96@gmail.com

March 2, 2022

ABSTRACT

The increasing electricity demand and the need for clean and renewable energy resources to satisfy this demand in a cost-effective manner, imposes new challenges on researchers and developers to maximize the output of these renewable resources at all times. However, the increasing penetration of renewable energy into the grid imposes new challenges on the grid operators. All of these challenges and issues gave rise to the need of Maximum Power Point Tracker (MPPT) and Flexible Power Point Trackers (FPPT) in order to maximize the power extracted from Photovoltaic (PV) systems and meet the grid operation constraints. Existing solutions for these algorithms do not take into consideration the very high dynamical nature of weather conditions that affects the output power that can be extracted from the PV modules, whereas in practice, the weather changes dynamically faster than what the algorithms time needed to converge. The work in this document is an attempt to address this shortcoming by utilizing online optimization algorithms for this purpose. Numerical analysis and verification are presented in the document. Code for the algorithms can be found at this link.

Keywords Flexible Power Point Tracking, Maximum Power Point, Photovoltaic Systems, Online Gradient Descent.

1 Introduction

Due to the rapidly increasing economies and businesses, in addition to the need for grid decarbonization to avoid the catastrophic consequences of climate change, renewable energy resources have seen a dramatic expansion in the power generating sector. Solar energy grew at a faster rate than other renewable energy sources, owing to its lower environmental effect and availability. In addition, due to the reduced cost of photovoltaic (PV) panels, the growth rate of installation of PV power plants (PVs) is rapidly increasing around the globe Staffell and Pfenninger [2018], Shen et al. [2021].

The most essential issue for both utility and residential PV owners is to maximize their revenue, which is dependent on cost and efficiency, thus it is necessary to maximize the extracted power. However, the maximum power that can be extracted at a time from the Pv is a function of irradiance, temperature and load, therefore the maximum operating power differs at each time and is unique. The change of irradiance, temperature or load changes the voltage at which maximum power transfer occurs and hence emerged the need for an algorithm that continuously tracks the maximum power point and operates the system at this point. These system or algorithms are known as Maximum Power Point Trackers (MPPT) Batarseh and Za'ter [2018], Khalane et al. [2017], in which a DC-Dc converter is implemented with a control algorithm in order to continuously change the duty cycle of the converter in order to match the source resistance (function of weather) to the load resistance (function of demand) as seen by the source.

However, the increased penetration of renewable energy into the grid and power system, poses new operational challenges that are largely related to the stability and reliability of the power system. Therefore, new constraints and operational regulations are being put into place to fulfil the future’s grid stability and power quality requirements and as a result, the concept of Flexible Power Point Tracking (FMPPT) has emerged posing a new challenges tracking algorithms as it can be seen in figure 1 Tafti et al. [2020].

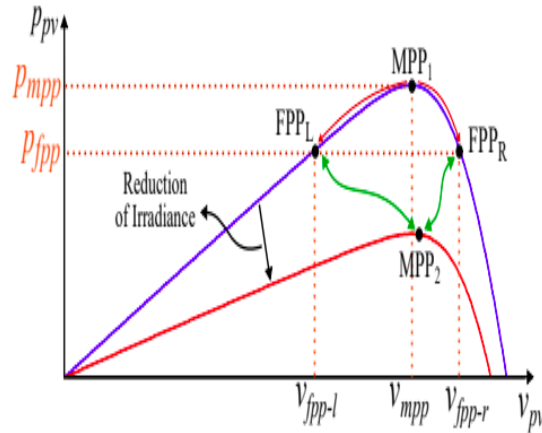


Figure 1: Maximum and flexible power point tracking in PVs (MPP -Maximum power point FPP - Flexible power point)Tafti et al. [2020]

This work proposes the use of Online Projected Gradient Descent (OPGD) as an attempt to operate PV modules that are connected to the grid using the micro-inverter topology as shown in figure 2 Zeb et al. [2018].

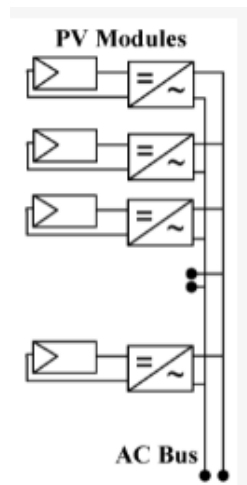


Figure 2: Ac modules (micro-inverter) topology Zeb et al. [2018]

The rest of the document is divided as follows: section II presents related work and the need for an online algorithm to solve the problem of FPPT. Section III illustrates the problem formulation, whereas section IV presents how OPGD is used to track the flexible power point. Section V presents the simulation setup and the results. Finally section VI presents the conclusion and practical implications of this work.

2 Time-Varying Constraints and Related Work

2.1 Time-Varying Constraints

Depending on the level of inverter-based resources penetration and the stability and reliability of the grid, different countries have various regulations and standards for the operation of PV system under different conditions. Different operational constraints impose different constraints that vary with time, weather conditions, load and other operational factors. The operational constraints are as follows Tafti et al. [2020], Peng et al. [2020]:

1. MPPT control zone (unconstrained). MPPT operation is implemented here, in which there are no operational constraints. The purpose of the algorithm in this zone is to extract the maximum available power from the PVs.
2. Power reserve constraint (delta power constraint). A delta power constraint is used to limit the active power from a PV to a desired constant value in a proportion of the maximum available power. This operational zone is important as a regulating reserve.
3. Ramp rate constraint. A ramp rate constraint is used to limit the power ramp rate by which the active power can be changed
4. Power limiting control (absolute power constraint). An absolute power constraint is typically used to protect the power system against overload in critical situations.

2.2 Related Work and The Need For Online Optimization

Maximum Power point tracking domain is older and hence more extensively explored than Flexible Power Point Tracking (FPPT). Therefore, to prove that FMMPT and MPPT tracking needs online optimization, MPPT literature will be considered as it is more rich and better documented. There are numerous MPPT algorithms in the literature, each of these algorithms has its strengths and drawbacks. However, the majority of the literature does not test these algorithms under rapidly changing weather conditions (mainly irradiance) and only focuses on accuracy and convergence time. However, irradiance variability is around $80 W/m^2$ in less than 2 seconds Lave and Kleissl [2010], Jain et al. [2020] and varies more with larger time steps. An $80 W/m^2$ change can contribute to a 6% loss in the power extracted if the operational point is remained unchanged. In addition to the weather, the load is continuously changing which also affects the optimal operation point. The algorithms in the literature usually consumes more time to converge to the maximum power point, which are summarized in the table below Bradai et al. [2017]:

Table 1: The performance of Algorithms in terms on convergence speed

Algorithm	Best Convergence	Worst Convergence
Fuzzy Logic Controller (FLC) Alajmi et al. [2011]	2.4 sec	5.4 sec
Particle Swarm Optimization (PSO) Lian et al. [2014]	6.59 sec	9.69 sec
Switched Photovoltaic Elserougi et al. [2015]	11.6 sec	16.8 sec
Artificial Bee Colony (ABC) Sundareswaran et al. [2014]	5.01 sec	5.63 sec

Therefore, as it can be seen from the table above, since the convergence time is less than the time it takes for the environmental conditions to change, there is a pressing need for an online algorithm.

3 Problem Formulation

As aforementioned, the purpose of Flexible Power Point Tracking (FPPT) is to maximize the overall power extracted from the PV modules under the different grid, load and operation constraints. However, the power available is continuously affected by the irradiance and temperature that affect the operation point of the PV that maximizes the available power at each time. Also, the current load affects the point of maximum operation. In this work, it is assumed that the irradiance at PV shown in figure 2 is uniform and equal (it is not necessarily uniform among all of the PV); meaning that partial shading conditions are outside the scope of this study as rarely occur under the micro-inverter topology.

The power extracted from a PV is given by equation (1):

$$P_{pv} = V * I_L - V * I_o * e^{\frac{V}{V_t}} \quad (1)$$

Where V is the voltage, I_L is the light generated current, I_o is the saturation current and V_t is the thermal voltage. The light generated current is a function of the irradiance, where is the thermal voltage V_t varies with the temperature of the module, which changes the power extracted and the required voltage V to operate at maximum power point.

For the purpose of this work, in order to treat the problem as a minimization instead of maximization problem, the power will be multiplied by -1. The flow of analysis is inspired by the work in Selvaratnam et al. [2018]

3.1 Preliminaries

Let $N := \{1, 2, \dots\}$ and $N_0 := N \cup \{0\}$. In this problem, F is considered the overall power in which $F := \{f_t : R^n | k \in N_0\}$ represents a family of continuous functions and where $X := \{X_t \subset R^n | t \in N_0\}$ are closed, non-empty sets that capture the possible time-varying constraints, and where n represents the number of PV modules that are connected to the grid. The algorithm is required to generate solutions to the following sequence of optimization problems as in equation (2):

$$\min_{x \in X_t} f_t(x) \quad (2)$$

using iteration of the form shown in equation (3):

$$x_{t+1} = G_t(x_t) \quad (3)$$

Where the operator $G_t : R^n \rightarrow R$ uses first-order information and knowledge of the feasible set X_t at the current time step.

In this work, uniform irradiance across the PV panels is assumed and hence it is safe to say the we are able to restrict attention to families of locally smooth, strongly convex functions with Lipschitz gradient and convex constraints, and hence we have the following assumptions:

Theorem 1 (Smoothness): Every $f \in F$ is twice continuously differentiable and therefore:

$$\exists L > 0, \|\nabla f(x) - \nabla f(y)\| \leq L\|x - y\|$$

Proof: Equation (1) shows that the power is an exponential function which are known to be smooth and are not globally Lipschitz continuous

Theorem 2 (Uniform strong convexity): There exists μ in which

$$\mu I \leq \nabla^2 f(x)$$

It is well documented and known in the literature that a PV under uniform irradiance has one unique maximizer (minimzer) and therefore strongly convex.

Assumption 1 (Convex Constraints): Every $X \in X$ is closed, convex and non-empty.

This work employs the online projected gradient descent algorithm to solve the problem presented in equation (2) which applies a certain choice for G_t that is shown in equation (3).

Let $P_x : R^n \rightarrow X$

$$P_x(y) := \arg \min_{x \in X} \|x - y\|^2$$

denote the projection operator, where $X \subset R^n$ is a closed, convex set. Projection guarantees the existence and uniqueness of $P_X(y)$. Projected gradient descent as in equation (4):

$$G_t(x) := P_{X_t}(x - \alpha_t \nabla f_t(x)) \quad (4)$$

where $\alpha_t > 0$ is the step size at time t.

Under assumption 2, f_t is guaranteed to have a unique global minimizer over X_t and the minimizer is defined as in equation (5):

$$x^* = \arg \min \{f_t(x) | x \in X_t\} \quad (5)$$

As a start to defining the general error bounds, the tracking error will be defined as in equation (6):

$$e_t = \|x_t - x_t^*\| \quad (6)$$

Tracking Error Dynamics

Let F, X satisfy assumptions 1-3, let $x_0 \in R^n$ and substituting equation (4) into (2), which results in the following:

$$x_{t+1} = P_{X_t}(x_t - \alpha_t \nabla f_t(x_t)) \quad (7)$$

where $\alpha_t < \frac{2}{L}$. Then, the convergence and tracking error are bounded as following:

$$\begin{aligned} \|x_{t+1} - x_{t+1}^*\| &= \|x_{t+1} - x_t^* + x_t^* - x_{t+1}^*\| \\ &\leq \|x_{t+1} - x_t^*\| + \|x_t^* - x_{t+1}^*\| \\ &\leq \rho_t \|x_t - x_t^*\| + \|x_t^* - x_{t+1}^*\| \end{aligned}$$

which finally results in:

$$\|x_{t+1} - x_{t+1}^*\| \leq \rho_t \|x_t - x_t^*\| + \|x_t^* - x_{t+1}^*\| \quad (7)$$

where $\rho_t = \max\{|1 - \alpha L_t|, |1 - \alpha \mu_t|\}$

As it can seen from equation (7), the tracking error is bounded by a dynamical system, where the shift in minimisers behaves as a disturbance input.

In order to have a steady-state error bound, the shift in minimizers (disturbance input or temporal variability) is assumed to be bounded, and hence assumption 4 is made accordingly.

Assumption 2 (Bounded change in minimiser) There exists $V \geq 0$ in which:

$$\|x_{t+1}^* - x_t^*\| \leq V$$

Corollary With the bound of the tracking error and the temporal variability for $\alpha < \frac{2}{L}$ then the following equation (8) holds:

$$\lim_{t \rightarrow \infty} \sup e_t \leq \frac{V}{1 - \rho} \quad (8)$$

Satisfying the bound in temporal variability, and from (7) and (8) it can be concluded that minimising ρ_t results in the fastest convergence rate and with a constant step size of $\alpha = \frac{2}{L + \mu}$. This yields the following bound:

$$\lim_{t \rightarrow \infty} \sup e_t \leq \frac{V(L + \mu)}{2\mu} \quad (9)$$

3.2 Metrics

In this work, The following metrics will be used to evaluate the performance of the algorithm:

1. **Tracking Error:** $\|x_t - x_t^*\|$ which represents the difference between the estimated voltage and the actual voltage at MPP.

2. **Instantaneous regret** $f_t(x_t) - f_t(x_t^*)$ which represents the difference between the output power and the maximum available power at time t and hence it represents the power lost. In the context of FPPT, the instantaneous power is greater than zero.
3. **Average Dynamic Regret** $\sum_{t=1}^T f_t(x_t) - \sum_{t=1}^T f_t(x_t^*)$ which represents the average power between the algorithms resulting output power and the maximum power available. It is useful to compute the dynamic regret as if multiplied by the operational time, it represents the overall energy lost and therefore it is important to compute the dynamic regret.
4. **Static Regret:** $\sum_{t=1}^T f_t(x_t) - \min_{x \in X} \sum_{t=1}^T f_t(x_t^*)$ Since there exists a tracking algorithm that is called constant voltage which fixes the operational voltage at a certain value and does not change it. Therefore it is important to compute the static regret.

The instantaneous regret is defined as in equation (10):

$$\phi_t = f_t(x_t) - f_t(x_t^*) \quad (10)$$

3.3 Unconstrained Case

First of all, bounds for the unconstrained case (MPPT control) are considered. The guarantee that $\nabla f_t(x_t^*) = 0$ when $X_t = R^n$ leads to the inequality in (11):

$$f_t(x_t) - f_t(x_t^*) \leq \frac{L}{2} e_t^2 \quad (11)$$

Consequently, instantaneous regret is bounded as following when $\alpha = \frac{2}{L+\mu}$ which is the value used to minimize the upper bound, then:

$$\lim_{t \rightarrow \infty} \phi_t \leq \frac{LV^2(L+\mu)^2}{8\mu^2} \quad (12)$$

3.4 Constrained Case

The previous error bounds apply equally well to constrained and unconstrained problems. However, the presence of constraints does mean that extra consideration should be taken into account. The bounds in the previous subsection do not apply as the minima does not have to be a stationary point.

Finite time feasibility: There exists

The following assumption of finite time feasibility guarantees feasibility of the projected gradient descent as following:

$$\|x_{t+1} - x_t^*\| \leq D \quad (13)$$

Where $D < +\infty$.

Bounds on the temporal variability:

$$\|x_{t+1}^* - x_t^*\| \leq \frac{V}{\mu}$$

Proof: To show the computation of the bound, starting from (derived in the previous problem):

$$\|x_t - x_t^*\| \leq \|x_t - x_{t-1}^*\| + \|x_{t-1}^* - x_t^*\|$$

Where f_t is strongly convex with μ .

Now substituting $x = x_{t+1}^*$ and using the fact that $\nabla f_{t+1}(x_{t+1}^*) = 0$ and adding it to the above, the equation becomes:

$$\|\nabla f_{t+1}(x_{t+1}^*) - \nabla f_t(x_{t+1}^*)\| \geq \mu \|x_{t+1}^* - x_t^*\|$$

And assuming that:

$$\|\nabla f_{t+1}(x_{t+1}^*) - \nabla f_t(x_{t+1}^*)\| \leq V$$

Then the bound is:

$$\|x_{t+1}^* - x_t^*\| \leq \frac{1}{\mu} \|\nabla f_{t+1}(x_{t+1}^*) - \nabla f_t(x_{t+1}^*)\| \leq \frac{V}{\mu} \quad (14)$$

Uniform Lipschitz cost for such $G \geq 0$, there exists:

For the pair F, X there exists $G > 0$ where

$$\|\nabla f_t(x)\| \leq G \quad (15)$$

Then we get the following inequality:

$$\phi_t \leq G e_t \quad (16)$$

for projected gradient descent and where $\alpha = \frac{2}{L+\mu}$, the bound on the instantaneous regret is as following,

$$\lim_{t \rightarrow \infty} \phi_t \leq \frac{GV(L+\mu)}{2\mu} \quad (17)$$

Dynamic regret bound:

With all the above definitions, and as aforementioned, the function is a sequence of a family of μ -strongly, smooth functions, and hence dynamic regret is bounded as in (18) Hazan [2019]:

$$Regret \leq \frac{G}{\mu} (1 + \log T) \quad (18)$$

4 Algorithms

This section presents the algorithms attempted to solve the FPPT problem explained earlier.

4.1 Proposed Online Algorithm

This work proposes the use of the online optimization method which is Online Projected Gradient Descent (OPGD). First of all, the sensors in the system takes the different relative measurements at each time; irradiance, temperature and load related values. Having the sufficient measurements, the power equation as in (1) can be calculated. Thus, the gradient with respect to the voltage can be calculated to get the optimal operating voltage, and finally the duty cycle of the DC-DC converter calculated accordingly to the optimal value that equalizes the load resistance as seen by the source resistance to the source resistance and thus achieving maximum power transfer. Figure 3 illustrates the flow of the algorithm.

Online projected gradient descent will be executed with a constant step size of $\alpha = \frac{2}{10}$.

4.2 Perturb and Observe

Perturb and Observe (P&O) is the most popular and widely used tracking algorithm for PV systems due to its relatively good accuracy, ease of implementation and being PV module independent. This work compares the performance of online gradient descent to the widely used P&O as a benchmark.

5 Simulation Results and Discussion

This section presents the simulation setup and associated simulation results.

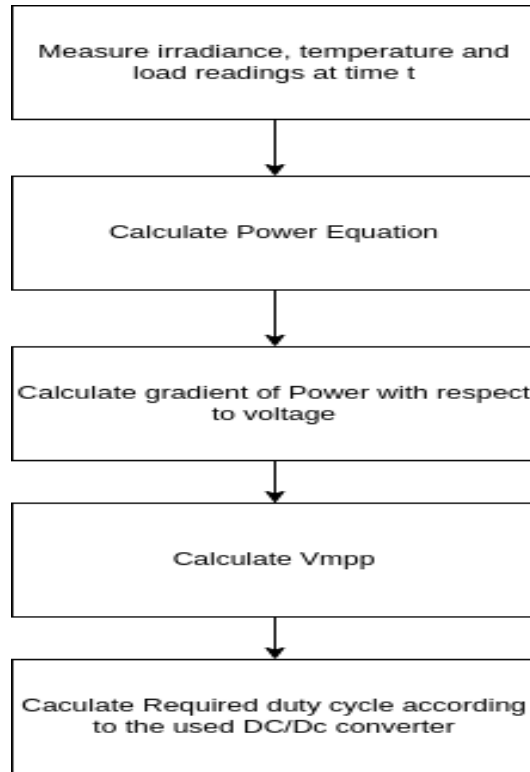


Figure 3: Online projected gradient descent algorithm flow

5.1 Simulation Setup

MATLAB Simulink is used as a simulation tool in order to build the following system configuration shown in figure 4. It is worth mentioning that for flexible power point tracking, the same controller will be used but with constraints on the operating conditions and thus has the same block diagram as below.

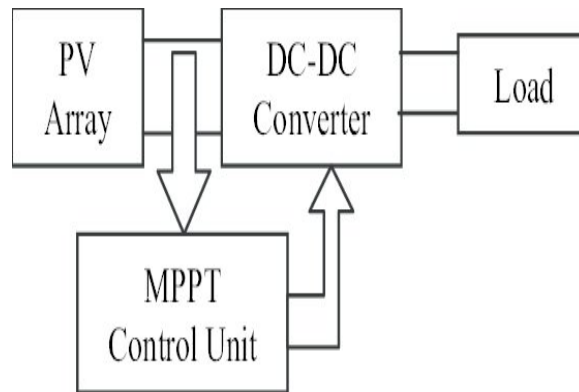


Figure 4: Maximum (flexible) Power Point block digram

For this work, a buck DC-DC converter is implemented, which has the following equation for duty cycle at maximum power point:

$$D_{mpp} = \sqrt{\frac{R_{output} * I_L - I_o * e^{\frac{V}{V_t}}}{V}} \quad (19)$$

Table 2 summarizes the characteristics of the PV modules used

Table 2: PV modules characteristics

PV Characteristic	Value
Number of modules	8
Open Circuit Voltage	36.3 V
Short Circuit Current	7.84 A
MPP Voltage at STC	29.2 V
MPP current at STC	7.3 A
Maximum Power at STC	213.15 W

Finally, the algorithms were tested under a highly fluctuating irradiance to test their ability to track the optimal operating point. The code and simulation files are available at this link.

5.2 Simulation Results

5.2.1 Unconstrained Case

Figures 5 and 6 below show the plots of the tracking and instantaneous errors respectively for the online gradient descent algorithm (the P&O graphs for clarity). Each time t is a 0.1 second step.

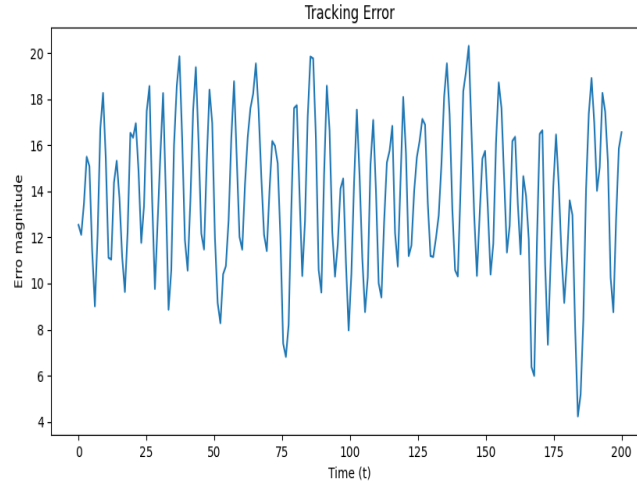


Figure 5: Tracking error - Unconstrained case

For further evaluation and comparison, the average dynamic regret and static regret are calculated for both the online gradient descent and P&O. For static regret, the operating voltage was simply fixed at 29 V. Table 3 presents the results for each algorithm. The dynamic regret shown is at the end of the simulation (at time T).

Table 3: OGD and P&O comparison for the unconstrained case

Metric	OGD	P&O
Average Dynamic Regret	54.67	67.3
Static Regret	51.36	55.3

5.2.2 Constrained case

As aforementioned, sometimes the grid imposes some operational challenges that requires some actions from the PV controllers such as solar curtailment, power control or over-voltage protection, which in turn imposes constraints on the PV controllers. In the constrained case, the two cases, the operational mode is varied between MPPT case (unconstrained), over-voltage protection, and active power control. Figures 7 and 8 below show the plots of the tracking and instantaneous errors respectively for the online gradient descent algorithm in the unconstrained case. Each time t is a 0.1 second step.

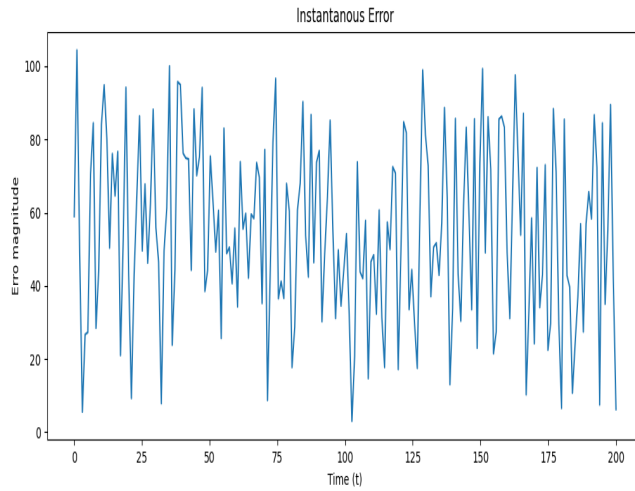


Figure 6: Instantaneous error - Unconstrained case

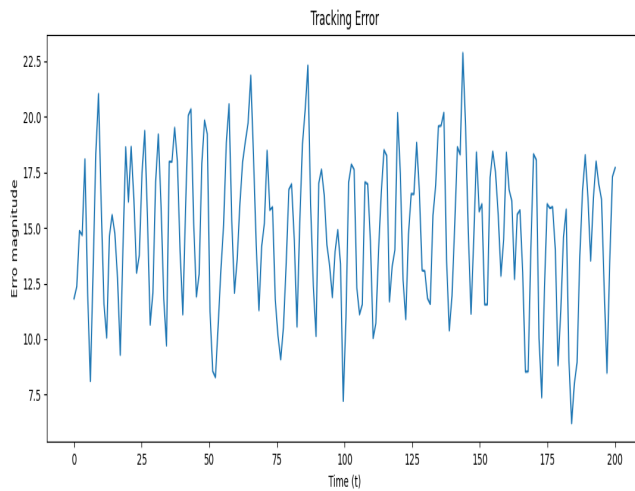


Figure 7: Tracking error - constrained case

Similar to the unconstrained case, the average dynamic regret and static regret are calculated and compared against the P&O as shown in table 4. It is worth mentioning that in the case of static regret, if the fixed operating voltage is above the constraint, it is then reduced to the allowed value. The dynamic regret shown is at the end of the simulation (at time T).

Table 4: OGD and P&O comparison for the constrained case

Metric	OGD	P&O
Average Dynamic Regret	61.363	72.4
Static Regret	55.1	57.41

6 Conclusion and practical implications

As there are 8 PV modules, with each module able to generate 213.15 W under Standard Test Conditions (STC) (1000 W/m^2 irradiance and 25 C temperature). The average loss of power for OGD for the unconstrained case is 54.7 W and

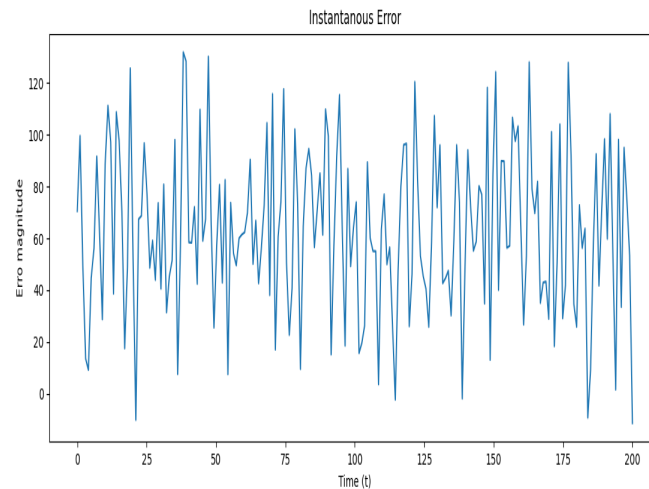


Figure 8: Instantaneous error - constrained case

61.36 for the constrained case. Whereas the P&O algorithm performance was relatively worse achieving 67.3 W and 72.4 W loss of power in the unconstrained and constrained cases respectively. However, on the span of time, the energy yielded from the OGD will be considerably higher than the energy harvested by the P&O. Also, it has been noticed, that when the sudden change in irradiance or load is high, the P&O performance becomes significantly worse, as it has to search for the MPP, which is usually much further from the original operating point. On the other hand, OGD is not affected by the variability in irradiance, as it actually calculates the required duty cycle and operating voltage rather than searching for it. Therefore, the OGD is better at placing the FPP under extreme varying conditions.

References

- Iain Staffell and Stefan Pfenninger. The increasing impact of weather on electricity supply and demand. *Energy*, 145: 65–78, 2018.
- Bo Shen, Fredrich Kahrl, and Andrew J Satchwell. Facilitating power grid decarbonization with distributed energy resources: Lessons from the united states. *Annual Review of Environment and Resources*, 46, 2021.
- Majd Ghazi Batarseh and Muhy Eddin Za’ter. Hybrid maximum power point tracking techniques: A comparative survey, suggested classification and uninvestigated combinations. *Solar Energy*, 169:535–555, 2018.
- Prasad S Khalane, Dattatray A Patil, and C Remadevi. Literature survey of various maximum power point tracking techniques for photovoltaic systems. In *2017 International Conference on Intelligent Computing, Instrumentation and Control Technologies (ICICICT)*, pages 836–840. IEEE, 2017.
- Hossein Dehghani Tafti, Georgios Konstantinou, Christopher D Townsend, Glen G Farivar, Ariya Sangwongwanich, Yongheng Yang, Josep Pou, and Frede Blaabjerg. Extended functionalities of photovoltaic systems with flexible power point tracking: Recent advances. *IEEE Transactions on Power Electronics*, 35(9):9342–9356, 2020.
- Kamran Zeb, Waqar Uddin, Muhammad Adil Khan, Zunaib Ali, Muhammad Umair Ali, Nicholas Christofides, and HJ Kim. A comprehensive review on inverter topologies and control strategies for grid connected photovoltaic system. *Renewable and Sustainable Energy Reviews*, 94:1120–1141, 2018.
- Qiao Peng, Ariya Sangwongwanich, Yongheng Yang, and Frede Blaabjerg. Grid-friendly power control for smart photovoltaic systems. *Solar Energy*, 210:115–127, 2020.
- Matthew Lave and Jan Kleissl. Solar variability of four sites across the state of colorado. *Renewable Energy*, 35(12): 2867–2873, 2010.
- Himanshu Jain, Manajit Sengupta, Aron Habte, and Jin Tan. Quantifying solar pv variability at multiple timescales for power systems studies. In *2020 47th IEEE Photovoltaic Specialists Conference (PVSC)*, pages 0180–0185. IEEE, 2020.
- Rafik Bradai, Rachid Boukenoui, Ahmed Kheldoun, Hassen Salhi, Malek Ghanes, Jean-Pierre Barbot, and Adel Mellit. Experimental assessment of new fast mppt algorithm for pv systems under non-uniform irradiance conditions. *Applied energy*, 199:416–429, 2017.

- Bader N Alajmi, Khaled H Ahmed, Stephen J Finney, and Barry W Williams. A maximum power point tracking technique for partially shaded photovoltaic systems in microgrids. *IEEE Transactions on Industrial Electronics*, 60(4):1596–1606, 2011.
- KL Lian, JH Jhang, and IS Tian. A maximum power point tracking method based on perturb-and-observe combined with particle swarm optimization. *IEEE journal of photovoltaics*, 4(2):626–633, 2014.
- Ahmed A Elserougi, Mohamed S Diab, Ahmed M Massoud, Ayman S Abdel-Khalik, and Shehab Ahmed. A switched pv approach for extracted maximum power enhancement of pv arrays during partial shading. *IEEE Transactions on Sustainable Energy*, 6(3):767–772, 2015.
- Kinattungal Sundareswaran, Peddapati Sankar, P Srinivasa Rao Nayak, Sishaj P Simon, and Sankaran Palani. Enhanced energy output from a pv system under partial shaded conditions through artificial bee colony. *IEEE transactions on sustainable energy*, 6(1):198–209, 2014.
- Daniel D Selvaratnam, Iman Shames, Jonathan H Manton, and Mohammad Zamani. Numerical optimisation of time-varying strongly convex functions subject to time-varying constraints. In *2018 IEEE Conference on Decision and Control (CDC)*, pages 849–854. IEEE, 2018.
- Elad Hazan. Introduction to online convex optimization. *arXiv preprint arXiv:1909.05207*, 2019.